Title: ERK1/2 Activation in Macrophages Promotes *Leishmania* Internalization and Pathogenesis

Running title: ERK1/2 facilitates *Leishmania* pathogenesis

Authors: Umaru Barrie[1, 2], Katherine Floyd[1, †], Arani Datta[1], and Dawn M. Wetzel[1, 3*]

Affiliations: [1]Department of Pediatrics, University of Texas Southwestern Medical Center, 5323 Harry Hines Blvd, Dallas, Texas, 75390, United States; [2]Medical Scientist Training Program, University of Texas Southwestern Medical Center, 5323 Harry Hines Blvd, Dallas, Texas, 75390, United States; [3]Department of Biochemistry, University of Texas Southwestern Medical Center, 5323 Harry Hines Blvd, Dallas, Texas, 75390, United States.

*Corresponding author: Dawn M. Wetzel, M.D., Ph.D.
Departments of Pediatrics (Infectious Diseases) and Biochemistry
The University of Texas Southwestern Medical Center, Dallas, TX 75019
Phone: 214-645-9510; Email: Dawn.Wetzel@UTSouthwestern.edu

[†]**Current address:** Department of Internal Medicine and Molecular Microbiology, Washington University School of Medicine, 660 S Euclid Ave, St. Louis, MO 63110, United States

Keywords: *Leishmania*, kinase, MAPK/ERK, parasite, macrophage

Abbreviations: BCA, Bicinchoninic acid; BMDM, bone marrow-derived macrophages; CC, cytotoxic concentration; CR3, complement receptor 3; FcγR, Fc gamma Receptor; h, hour; IC, inhibitory concentration; IL, Interleukin; INFγ, Interferon gamma; Mϕ, macrophage; m, minutes; MAPK/ERK, Mitogen-activated protein kinases/Extracellular signal regulated kinases; PKC, Protein Kinase C; PVDF, polyvinylidene difluoride; RAF, Rapidly Accelerated Fibrosarcoma; RIPA, radioimmunoprecipitation assay; p-, phosphorylated; PMA, Phorbol 12-myristate 13-acetate; SD, standard deviation; SFK, Src family kinases; SYK, spleen tyrosine kinase; TNF, Tumor Necrosis Factor

This file includes:

Abstract word count: 219

Summary statement character count: 141

Manuscript word count: 9,549

Number of references: 57

Number of figures: 6

Number of tables: 2

Supplemental figures: 1

Supplemental tables: 3

ABSTRACT: The obligate intracellular protozoan parasite *Leishmania* binds several host cell receptors to trigger its uptake by phagocytic cells, ultimately resulting in visceral or cutaneous leishmaniasis. After *Leishmania* engages receptors on macrophages and other phagocytes, a series of signaling pathways in the host cell are activated during its internalization, which are critical for establishment and persistence of *Leishmania* infection. Thus, preventing *Leishmania* internalization by phagocytes could be a novel therapeutic strategy for leishmaniasis. However, the host cellular machinery that mediates promastigote and amastigote uptake is poorly understood. Here, using small-molecule inhibitors of Mitogen-activated protein kinases/Extracellular signal regulated kinases (MAPK/ERK), we demonstrate that ERK1/2 mediates efficient *Leishmania amazonensis* uptake and phagocytosis of beads by macrophages. We find that inhibition of MEK1/2 or ERK1/2 leads to inefficient amastigote uptake by macrophages. Moreover, using inhibitors and primary macrophages lacking spleen tyrosine kinase (SYK) or Abl family kinases, we show that SYK and Abl family kinases mediate Raf, MEK, and ERK1/2 activity and are necessary for efficient uptake. Finally, we demonstrate that trametinib, a MEK1/2 inhibitor used clinically to treat certain cancers, significantly reduces disease severity and parasite burden in *Leishmania*-infected mice, even if it is started after lesions develop. Our results show that maximal *Leishmania* infection requires MAPK/ERK and highlight the potential for MAPK/ERK-mediated signaling pathways to be novel therapeutic targets for leishmaniasis.

69 **One sentence summary**: An Abl2-SYK-Raf-MEK-ERK pathway facilitates

70 *Leishmania* uptake by phagocytic cells and promotes disease severity in

71 *Leishmania*-infected mice.

72

Main text:

INTRODUCTION

Leishmania spp. are obligate intracellular, protozoan parasites spread by the sand fly vector (*1*), causing leishmaniasis, a group of diseases ranging from self-healing cutaneous ulcers (*2*) to deadly disseminated visceral disease (*3*). Leishmaniasis represents a major global health problem, since over 12 million people currently suffer from this disease. Approximately 2 million people are newly infected by *Leishmania* spp. annually (*4*). Moreover, it is estimated that over 350 million people in 98 countries worldwide are at risk of developing leishmaniasis (*4, 5*), and the disease is now spreading into previously non-endemic areas, including the United States (*6, 7*). *Leishmania*, particularly the species causing cutaneous disease, are understudied, and current treatments are few, expensive, poorly effective, and toxic. Resistance is also emerging (*8-11*). Thus, identifying new drugs with novel mechanisms of action that circumvent resistance mechanisms is an urgent priority for effective drug development.

When an infected sand fly encounters its host, *Leishmania* promastigotes must be internalized by phagocytic cells such as macrophages (Mϕ) in order to persist in the host (*12, 13*). This process is then repeated as the mammalian life cycle stage, the amastigote, replicates and spreads to other phagocytic cells to cause pathogenesis (*14*). Based on prior studies, the Fcγ classes of receptors (FcγR) are the primary receptor on the host cell surface that permit amastigote uptake (*14*). Major advancements have been made in understanding the

96 immunomodulatory events involved in the pathogenesis of leishmaniasis.
97 However, little is known about the basic molecular events underlying the
98 signaling events, especially the host cellular pathways, which facilitate the
99 receptor-mediated uptake of *Leishmania* by Mϕ and other phagocytes.
100
101 Our previous studies have identified the Src (*15*) family kinases (SFK, and
102 specifically Hck, Fgr, and Lyn), Abl1 (Abl) and Abl2 (Arg) (*16*) kinases, and
103 Spleen Tyrosine Kinase (SYK) (*17*) as major protein families involved in
104 phagocytosis. Specifically, we have demonstrated that Abl facilitates
105 complement-mediated phagocytosis, and Arg enhances immunoglobulin/ FcγR-
106 mediated phagocytosis (*15, 16*). Modulation of these kinases via genetic
107 manipulation or small molecule inhibitors abrogates *L. amazonensis*
108 internalization by Mϕ, and thus limits disease progression in mice (*15-17*).
109 However, our studies also indicate that these kinases have a limited role in the
110 host's immune response to *Leishmania* or parasite clearance (*15-17*). A drug that
111 simultaneously decreases parasite uptake, limits parasite survival, and promotes
112 immunological responses that are advantageous to the host could provide added
113 advantages to reduce infection and disease burden. Host-cell active agents could
114 also theoretically be used to combat other intracellular pathogens that employ
115 similar uptake mechanisms.
116
117 Exactly how SFK, Abl family kinases, and SYK would regulate the events that
118 occur during *Leishmania* uptake and phagocytosis has not been fully established.

119 Others and we have demonstrated that CrkII is activated after signals have been
120 relayed from SFK to Arg to SYK, leading to actin-rich phagocytic cup formation
121 and pathogen uptake (*15-18*). Interestingly, studies have been published in
122 cancer model systems indicating that Src (*19*), Abl family kinases, and SYK (*20,*
123 *21*) also can activate MAPK/ERK signaling. However, it is not clear whether
124 MAPK/ERK signaling would play a role in phagocytosis. Nevertheless,
125 MAPK/ERK are known to directly phosphorylate cytoplasmic or nuclear proteins,
126 including transcription factors, that control several fundamental cellular
127 processes from proliferation and differentiation to innate and adaptive immune
128 responses (*22-24*). In addition, Phorbol 12-myristate 13-acetate (PMA) is known
129 to activate MAPK/ERK through protein kinase C (PKC) (*25*). Previous studies
130 have shown that MAPK/ERK signaling modulates the immune response to
131 *Leishmania* infection to favor chronic infection and survival of the parasite inside
132 phagocytic cells (*26-30*). Correspondingly, inhibiting MEK1/2 with PD98059 has
133 been shown to enhance *L. amazonensis* killing by activating reactive oxygen
134 species (ROS) and repressing IL-10 production (*18, 31-33*). These results
135 directly implicate ERK1/2 phosphorylation as a mechanism through which the
136 parasite promotes persistence and subverts the immune response (*18*).
137 However, experiments characterizing early time points in the *Leishmania* life
138 cycle, during the uptake of these parasites by Mϕ, have not been conducted.
139
140 Here, we uncover a new role for MAPK/ERK during *Leishmania* internalization and
141 pathogenesis. We show that Raf-1, MEK1/2, and ERK1/2 activities are induced

142 following infection and are necessary for efficient uptake of amastigotes. Host
143 MAPK/ERK is activated by Arg and SYK to facilitate this process. In combination
144 with prior results (*15-18*), our molecular studies elucidate an FcγR-SFK-Arg-SYK-
145 Raf-MEK-ERK signaling relay as a major pathway involved in establishment of
146 leishmaniasis by facilitating parasite uptake. In addition, using a mouse model, we
147 establish that MAPK/ERK are required for the development and worsening of lesions
148 in cutaneous leishmaniasis. Of particular interest, targeting MAPK/ERK with specific
149 inhibitors limits leishmaniasis manifestations and parasite burden in mice, even
150 when these inhibitors are started after lesions are apparent. Our experiments
151 highlight MAPK/ERK inhibitors as potential new treatment modalities for this
152 devastating disease.
153

154 **RESULTS**

155 **MAPK/ERK signaling in Mϕ facilitates *Leishmania* uptake**

156 To directly test whether the MAPK/ERK pathway mediates *Leishmania* uptake,
157 we first explored the effect of the MEK1/2 inhibitor trametinib on the uptake of *L.*
158 *amazonensis*. We can grow both promastigotes and amastigotes of this species
159 in tissue culture without host cells (*i.e.*, axenic culture), which facilitates our
160 studies of *Leishmania* uptake by Mϕ. Trametinib is a highly selective and potent
161 MEK1/2 inhibitor, with an IC_{50} for the purified kinase ranging from 0.92 nM to 3.4
162 nM in cell-free assays (*34, 35*). It has no effect on the kinase activity of c-Raf, B-
163 Raf, or ERK1/2. We pretreated RAW 264.7 cells, a Mϕ–like cell line, for 2 hours
164 (h) with trametinib or imatinib, an Abl/Arg inhibitor with an IC_{50} of 100-500 nM in
165 kinase assays (*35*), as a positive control. We then added *Leishmania* to samples
166 to allow uptake. Trametinib decreased the uptake of IgG-opsonized amastigotes
167 in RAW 264.7 cells, comparable to the reductions seen after treatment with
168 imatinib (**Fig. 1A, B),** as demonstrated by a lower phagocytic index (PI), or
169 number of internalized parasites per 100 Mϕ. No differences were seen in the
170 total (external + internal) number of *Leishmania* per 100 RAW 264.7 cells, which
171 we term an adhesion index, among these conditions (**Fig. 1C**). We performed a
172 titration of trametinib's effects on amastigote uptake, and the maximal reduction
173 in PI was shown at 1 μM trametinib (**Fig. 1D, E**)**.** We also determined that over
174 72 h, the CC_{50} (cytotoxic concentration required to kill 50% of viable cells) for
175 RAW 264.7 cells was greater than our maximum concentration of 2.5 μM.
176 Internalization defects remained even after prolonged incubation in trametinib (up

177 to 240 minutes) and were not due to reduced adhesion, as amastigotes
178 continued to be bound to trametinib-treated RAW 264.7 cells at levels
179 indistinguishable from controls (**Fig. 1F, G**). Treating Mϕ with other MAPK/ERK
180 pathway inhibitors (*36*) such as selumetinib (which affects MEK1/2), PD0325901
181 (another MEK1/2 inhibitor), and SCH772984 (an ERK1/2 inhibitor), also
182 significantly reduced amastigote uptake without affecting adhesion
183 (**Supplemental Fig. 1A, B**). In addition, we found that treating RAW 264.7 cells
184 with the MEK1/2 inhibitor PD0325901 (*37*) decreased the internalization of
185 promastigotes, to a degree that was comparable to treatment with imatinib
186 (**Supplemental Fig. 1C, D**). Together, these results establish that targeting
187 MEK1/2 and ERK1/2 significantly attenuates internalization of both *L.*
188 *amazonensis* life cycle stages.
189
190 **cRaf, MEK1/2, and ERK1/2 are activated during amastigote uptake**
191 Having established that MAPK/ERK are important for *Leishmania* uptake, we
192 assessed whether kinases involved in this pathway were activated during
193 amastigote internalization. Raf-1 (cRaf), MEK1/2, and ERK1/2 are key members of
194 the MAPK/ERK pathway (*24, 38*). We thus measured cRaf, MEK1/2, and ERK1/2
195 phosphorylation in RAW 264.7 cells to examine the relative phosphorylation level of
196 each kinase during internalization of amastigotes. Essentially no phosphorylated
197 ERK or ERK was detected in amastigote samples (**Supplemental Fig. 1E**).
198 However, amastigotes potently induced ERK1/2 phosphorylation in Mϕ, with
199 phosphorylation levels increasing by 3 and 4.5-fold at 10- and 30-minutes post-

200 infection, respectively (**Fig. 2A**). Similarly, MEK1/2 (**Fig. 2B**) and cRaf (**Fig. 2C**)
201 were activated by amastigotes during infection**.** These data indicate that amastigotes
202 rapidly activate MAPK/ERK in a sustained fashion during their uptake by Mϕ.
203
204 **PMA rescues MAPK/ERK related uptake defects**
205 PMA is known to activate ERK1/2 through PKC, with an IC_{50} of 11.7 nM against
206 purified kinase (*25*). Therefore, we next investigated whether PMA affected
207 amastigote internalization. To perform these experiments, and to confirm our prior
208 results from a cell line using primary cells, we isolated bone marrow derived-Mϕ
209 (BMDM) from C57BL/6 mice. PMA-treated BMDM were able to internalize IgG-
210 coated amastigotes at higher levels than DMSO-treated BMDM in a dose-dependent
211 manner, reaching maximal internalization at 2.5 μM PMA (**Fig. 3A, B**). Importantly,
212 10 μM trametinib and 10 μM PMA did not affect growth of amastigotes in culture
213 (**Fig. 3C**), indicating that they do not exert their effects on internalization by acting
214 directly on *Leishmania*. Furthermore, PMA treatment rescued trametinib inhibition of
215 *Leishmania* uptake in BMDM to PI that were indistinguishable from those of DMSO-
216 treated controls (**Fig. 3D-F**). Collectively, our data indicate that ERK1/2 kinase
217 activity is necessary for maximal *Leishmania* uptake. In addition, although PKC
218 activation was seen during the uptake of amastigotes, PMA treatment increased
219 PKC activity in RAW 264.7 cells to 8-fold higher levels than during baseline
220 amastigote uptake (**Fig. 3G, H**).
221
222 **ERK1/2 is activated by Arg/Abl and SYK during amastigote uptake**

223 Next, we investigated the mechanism by which *L. amazonensis* amastigotes induced
224 ERK1/2 phosphorylation during their uptake. Previous research has shown that Arg
225 facilitates *Leishmania* amastigote uptake downstream of SFK (*15*). In addition,
226 inhibition of SYK, a tyrosine kinase implicated in FcγR immunoglobulin-mediated
227 signaling (*17, 18, 39, 40*) reduces ERK1/2 activation in a dose-dependent manner in
228 other systems (*18, 41*). To test for roles for these kinases, small molecule inhibitors
229 (imatinib, entospletinib [IC_{50} for activity against purified SYK = 7.7 nM] (*41*),
230 SCH772984, trametinib), and ERK1/2 activator PMA (*25*) were added to RAW 264.7
231 cells before infection with amastigotes. Inhibition of Arg and SYK with imatinib and
232 entospletinib, respectively, significantly reduced ERK1/2 phosphorylation, to a
233 similar degree to the MAPK/ERK inhibitors SCH772984 and trametinib (**Fig. 4A, B**).
234 As expected, PMA, the positive control, significantly increased ERK1/2
235 phosphorylation. Furthermore, addition of 1 μM PMA to trametinib-treated cells
236 rescued inhibition of ERK1/2 phosphorylation to DMSO/control levels. The inhibitors
237 and activators followed similar trends for promastigote-induced ERK activity
238 (**Supplemental Fig. 1F**). Thus, we could modulate *Leishmania*-induced ERK activity
239 by both inhibitors and activators *in vitro*.
240
241 To further study the role of SYK and Arg in *Leishmania*-induced ERK
242 phosphorylation, we next isolated BMDMs from mice lacking Abl family kinases
243 (*Arg*$^{-/-}$*Abl*$^{flox/flox}$*LysM Cre*$^{+}$ [termed *Arg*$^{-/-}$*Abl*$^{-/-}$ when discussing isolated BMDM]),
244 SYK (*SYK*$^{flox/flox}$ *Cre*$^{+}$, abbreviated *SYK*$^{-/-}$ when referring to isolated BMDM) or wild
245 type (*WT*) littermates. We have previously shown that amastigote uptake is

246 dependent upon Arg but not Abl (*15-16*). Our immunoblots showed *Arg*$^{-/-}$*Abl*$^{-/-}$ and
247 *SYK*$^{-/-}$ BMDM nearly completely lack Arg or SYK, respectively, while ERK1/2
248 expression was maintained (**Supplemental Fig. 1G**). Consistent with our chemical
249 inhibition experiments, SYK$^{-/-}$ and *Arg*$^{-/-}$*Abl*$^{-/-}$ BMDM limited amastigote-mediated
250 ERK1/2 phosphorylation, demonstrating that SYK and Arg/Abl are necessary for
251 stimulating ERK1/2 phosphorylation following engagement of the FcγR (**Fig. 4C, D**).
252 At low doses (250 nM), PMA rescued ERK1/2 activity in *Arg*$^{-/-}$*Abl*$^{-/-}$ and *SYK*$^{-/-}$
253 BMDM. This suggested 1) amastigotes operate through a distinct pathway to
254 activate ERK1/2 compared to PMA, which activates MAPK/ERK through PKC (*25*)
255 and 2) during FcγR immunoglobulin-mediated amastigote infection, Arg and SYK
256 family kinases are upstream of MAPK/ERK and are necessary to activate the
257 MAPK/ERK pathway.
258
259 To directly test whether Arg is critical for ERK1/2-mediated amastigote uptake, we
260 treated *WT* and *Arg*$^{-/-}$*Abl*$^{-/-}$ BMDM with DMSO or PMA prior to infection with IgG-
261 opsonized amastigotes. We found that *Arg*$^{-/-}$ *Abl*$^{-/-}$ BMDM displayed defects in IgG-
262 mediated amastigote uptake, while PMA treatment partially rescued these defects
263 (**Fig. 4E-G**), returning uptake to 66.4 ± 16.6% (mean ± SD) compared to 29.3 ± 0.9%
264 with DMSO. Similarly, SYK was necessary for efficient amastigote uptake, and the
265 decreased PI of *SYK*$^{-/-}$ BMDM was partially rescued by PMA treatment
266 (**Supplemental Fig. 1H, I**). Taken together, these results, in combination with prior
267 data, are consistent with a signaling pathway in which Arg/Abl and SYK act

268 upstream of and activate the ERK1/2 pathway (which is at least partly independent
269 from PKC) to facilitate amastigote uptake (*25*).
270
271 **MAPK/ERK inhibition minimally impacts phagocytosis of opsonized beads**
272 *Arg*$^{-/-}$ BMDM have been shown to have impaired phagocytosis overall, as
273 demonstrated using IgG-coated (opsonized) beads (*16*). Thus, we hypothesized that
274 the Arg-SYK-ERK pathway may be necessary for the general process of
275 phagocytosis, in addition to amastigote uptake. To delineate the specific
276 contributions of MAPK/ERK to phagocytosis, we examined bead uptake compared
277 to amastigote uptake by RAW 264.7 cells. Surprisingly, phagocytosis of IgG-
278 opsonized beads by RAW 264.7 cells was less affected by trametinib (**Fig. 5A, B**) or
279 SCH772984 (**Supplemental Fig. 1J, K)** compared to the uptake of IgG-coated
280 amastigotes (**Fig. 1)**. However, no differences in phagocytosis of IgG-opsonized
281 beads versus amastigotes were observed when RAW 264.7 cells were treated with
282 imatinib, suggesting that Arg/Abl play a more generalized role in phagocytosis.
283 Collectively, these data suggest that ERK1/2 activation is important for *Leishmania*
284 uptake specifically but may play a minor role in standard phagocytic mechanisms.
285
286 We also tested whether MAPK/ERK activity was differentially induced following
287 addition of beads compared to amastigotes. Beads induced ERK1/2 phosphorylation
288 in a time-dependent fashion, such that activation reached maximal levels between 5
289 and 10 m and ERK1/2 phosphorylation was not detectable after 30 m (**Fig. 5C, D**).
290 Similarly, beads activated upstream kinases MEK1/2 and cRaf; however, their

291 phosphorylation was not sustained (**Fig. 5E-H**). Thus, in contrast to the sustained
292 activation of MAPK/ERK that we saw during amastigote uptake, beads had only a
293 transient effect on ERK1/2 activation.
294
295 **Trametinib decreases lesion size and parasite burden in a murine model of**
296 **cutaneous leishmaniasis.** To test whether the MAPK/ERK pathway is necessary
297 for *Leishmania* pathogenesis *in vivo*, we employed a C57BL/6 mouse model of
298 cutaneous leishmaniasis using *L. amazonensis.* Footpad swelling (*i.e*., lesion size)
299 was measured in infected mice treated with 2 mg/kg of body weight/day of oral
300 trametinib or drug vehicle (control) starting 7 days (d) before inoculation and
301 continuing for the experimental duration of 14-16 weeks (*15, 16*) (**Fig. 6A**).
302 Compared to controls, trametinib-treated mice had smaller lesions develop (**Fig.**
303 **6B**), which contained fewer parasites in lesions (**Fig. 6C**). The decreased number of
304 parasites found within lesions may help to explain these changes in lesion size.
305
306 Overall, in leishmaniasis, a Th1 response is thought to be beneficial to the host,
307 while a Th2 response is thought to be deleterious. To determine whether the
308 immunological effects of MEK1/2 inhibition were associated with the healing seen
309 in trametinib-treated mice, we isolated draining lymph nodes from infected DMSO
310 and trametinib-treated mice. We then profiled cytokine and chemokine secretion
311 after stimulation with high (1×10^6) or low (1×10^5) doses of parasite lysates (*42,*
312 *43*) compared to unstimulated. A mild shift in the overall ratio of Th1 to Th2
313 cytokines (Th1/Th2) towards a Th2 phenotype in trametinib-treated mice was

314 seen (**Table 1**), which should be deleterious to the host. Notably, lymph nodes
315 extracted from trametinib-treated mice released lower quantities of cytokines in
316 response to *L. amazonensis* than those isolated from diluent-treated animals
317 (**Table 2**). Trametinib-treated mice also demonstrated decreased cytokine
318 production in response to concanavalin A (Con A) stimulation. In addition, we
319 assessed chemokine secretion following MEK1/2 inhibition. Of interest, the
320 production of several chemokines implicated in *Leishmania* pathogenesis,
321 including MIP-1α (CCL3) and MCP-1 (CCL2), were significantly decreased with
322 trametinib (**Table 2**), consistent with the decrease in cytokines/chemokines
323 overall.
324
325 We further tested whether MEK1/2 inhibition with trametinib reduces pathogenesis
326 after the development of symptoms by infecting mice as above. However, we started
327 diluent vs trametinib at 6 weeks after inoculation (*i.e.*, once lesions were visible) and
328 continued therapy for the remaining experimental duration (**Fig. 6D**). Remarkably,
329 even with delayed treatment, trametinib-treated mice reproducibly had smaller
330 lesions (**Fig. 6E**). They also had significantly lower parasite burdens than those of
331 controls (**Fig. 6F**), which at least in part may explain these results. We also saw
332 similar immunological responses in mice treated with trametinib that was initiated
333 partway through the experiment as we did for the mice treated prior to *Leishmania*
334 infection (**Supplemental Table 1, Supplemental Table 2**). Overall, our findings
335 demonstrate that trametinib administration limits the manifestations of leishmaniasis
336 in a mouse model, even if it is initiated after lesions develop.

337 **DISCUSSION**

338 Here, we have shown that efficient *Leishmania* uptake by Mϕ and infection in mice
339 requires MAPK/ERK. While previous studies have shown that ERK1/2 activation
340 post-infection by *Leishmania* alters various host signaling pathways, leading to
341 increased intracellular survival and replication of these parasites (*33, 44*), our results
342 establish an earlier role for host ERK1/2 activity during the *Leishmania* life cycle, and
343 show that ERK1/2 is necessary for *Leishmania* uptake into Mϕ. In combination with
344 prior data, we propose a model whereby, following engagement of the FcγR, host
345 Arg/Abl and SYK stimulate Raf, MEK, and ERK1/2 phosphorylation, leading to
346 amastigote uptake (**Fig. 6G**). Moreover, *in vivo* inhibition of MEK1/2 by trametinib in
347 a mouse model of cutaneous leishmaniasis significantly limits lesion development
348 and parasite burden, even when trametinib is started after these lesions are visible.
349 Our results highlight a critical role for MAPK/ERK signaling in *Leishmania* uptake
350 and pathogenesis.

351

352 Our data indicate that Arg/Abl and SYK are required for amastigote-mediated
353 ERK1/2 phosphorylation following FcR receptor activation. Our prior studies of host
354 signaling required for *Leishmania* uptake revealed that amastigotes bind directly to
355 FcγR (*45*) and activate SFK-Arg pathways (*15*) to induce uptake. We conclude from
356 our combined results that a FcR-SFK-Arg-SYK signaling pathway functions
357 upstream of and activates MAPK/ERK family kinases. Interestingly, pharmacological
358 inhibition of MEK1/2 and ERK1/2 in RAW 264.7 cells significantly reduces, but does
359 not completely abolish, *Leishmania* uptake. One possible explanation for these

360 results is that kinase inhibition via these compounds is incomplete. Another is that
361 *Leishmania* uptake is likely mediated via additional host signaling pathways.
362 Supporting the latter, we find that low or sub-EC_{50} doses of PMA, which activates
363 ERK1/2 through an SFK-Arg-SYK-independent manner, rescues trametinib inhibition
364 of *Leishmania* amastigote uptake in RAW 264.7 cells, and in *SYK*$^{-/-}$ and *Arg*$^{-/-}$*Abl*$^{-/-}$
365 BMDM. PMA is a known activator of PKC (*25, 46-50*). However, we find that PKC
366 activity is only slightly increased during amastigote infection of WT/DMSO-treated
367 Mϕ, suggesting that PKC may play only a minor role during typical amastigote
368 uptake. Ongoing work in the laboratory is directed at uncovering these additional
369 novel uptake mechanisms for *Leishmania*. In addition, although drug combinations
370 typically are not used to treat leishmaniasis, they are the standard of care for many
371 other infections, such as HIV or tuberculosis. Combination therapy with multiple
372 kinase inhibitors to inhibit several uptake pathways at once may provide additional
373 benefit for the treatment of leishmaniasis over single host cell kinase inhibitors
374 alone.
375
376 Our data using MEK/ERK inhibitors indicates that there are differences in
377 MAPK/ERK signaling within Mϕ depending on whether *Leishmania* amastigotes or
378 IgG-coated beads are undergoing internalization. These results differ from most
379 available literature that concludes that *Leishmania* primarily hijacks ongoing
380 phagocytic pathways to facilitate its uptake. We instead suggest that there may be
381 alternative, perhaps partly redundant, pathways that may support the uptake of
382 *Leishmania* over the phagocytosis of beads, and vice versa. Our future experiments

383 will compare and contrast the signaling pathways required for these different uptake
384 mechanisms between opsonized beads and *Leishmania* parasites.
385
386 Our experiments using a mouse model for *Leishmania* infection show that
387 MAPK/ERK are required for maximal *Leishmania* pathogenesis during cutaneous
388 leishmaniasis. Given that trametinib has no direct effect on parasite growth in
389 culture, one highly plausible explanation for the decreased lesion size and parasite
390 burden that we see in trametinib-treated mice is our previously documented
391 inhibition of *Leishmania* uptake. Consistent with this hypothesis, fewer parasites are
392 found in lesions from trametinib-treated mice than in control mice. Alternately, we
393 also considered that lesion size variations after *L. amazonensis* infection might result
394 from trametinib limitation of host inflammatory and immunological responses. Many
395 pathogens hinder immune responses by targeting host intracellular signaling
396 pathways, including MAPK pathways (*49, 51*). The murine immune response to
397 leishmaniasis is complicated and varies depending on the species of *Leishmania*
398 and the mouse strain used. As a simplified paradigm, Th1 responses are generally
399 protective, but Th2 responses are harmful to the host (*26, 29, 30*). We find that
400 cytokines assessed following *Leishmania* antigen stimulation in lymph nodes
401 isolated from infected trametinib-treated mice are reduced from the levels seen in
402 diluent-treated mice. One possible explanation is that fewer cytokines are generated
403 because the lesions contained fewer parasites. Another is that trametinib could
404 instead dampen pathways important for maintaining an active inflammatory
405 response to the ongoing host response to infection. Supporting this second

406 possibility, cytokines measured after Con A stimulation (an antigen-independent
407 mitogen used as an alternative T cell stimulus) are significantly reduced by MEK1/2
408 inhibition. Overall, the moderate shift in the total ratio of Th1 to Th2 cytokines
409 (Th1/Th2) toward a Th2 phenotype that we see theoretically should exacerbate
410 disease rather than alleviate it. Reduced levels of proinflammatory chemokines like
411 MIP-1 (CCL3) and MCP-1 (CCL2), on the other hand, may be responsible for
412 reducing lesion size by restricting the number of immune cells, especially phagocytic
413 cells, which reach the site of infection. Further work is needed to delineate the
414 regulation of immune responses to *Leishmania* infection and the resulting effects on
415 lesion worsening versus healing.
416
417 Finally, and of particular interest, we have demonstrated that there are reductions
418 in lesion size and parasite burden if trametinib therapy is used in the mouse
419 model of cutaneous leishmaniasis, even if it is started after foot swelling is
420 visible. Compared to our previous results, the data shown here strongly suggest
421 that trametinib reduces lesion size more than imatinib (*16*) or bosutinib (*15*),
422 which target signaling molecules in the same pathway. Trametinib is used
423 clinically as anti-cancer therapy, making it feasible that this drug could be
424 repurposed to treat an infectious disease, and facilitating potential clinical trials
425 for its use against leishmaniasis. Our data imply that inhibiting a signaling
426 pathway downstream of SFK-Arg-SYK might improve results over inhibiting
427 kinases upstream in the pathway. Our results also give credence to our
428 overarching hypothesis that targeting host cell pathways, particularly ones that

429 are required for multiple aspects of the parasite life cycle and pathogenesis, may
430 permit treatment of an infectious disease such as leishmaniasis.
431
432 In summary, we have demonstrated that Arg-SYK signaling through ERK1/2
433 facilitates IgG-mediated phagocytosis and *Leishmania* uptake. Furthermore, ERK
434 activity helps to govern the subsequent pathogenesis and disease progression of
435 leishmaniasis in the mouse model. Due to the specificity of MAPK/ERK small
436 molecule inhibitors, it is possible to selectively target MEK1/2 and ERK1/2 for
437 potential therapeutic intervention. Our findings demonstrate the significance of
438 MAPK/ERK signaling during *Leishmania* entry into phagocytic cells and suggest
439 innovative therapeutic methods for leishmaniasis. Our future studies will investigate
440 the use of host-cell-active drugs, potentially in conjunction with other kinase
441 inhibitors or existing antiparasitics, to improve efficacy, decrease toxicity, and limit
442 the likelihood of developing resistance. Furthermore, our results support the novel
443 possibility that medications that target conserved host cell processes rather than
444 infectious pathogens might be employed to treat a wide spectrum of intracellular
445 pathogens.
446
447

448 **MATERIALS AND METHODS:**

449 **Mice.** C57BL/6 mice were procured from Jackson Laboratory (Bar Harbor, ME).
450 *Syk*$^{flox/flox}$ *Cre*$^{+}$ and *Arg*$^{-/-}$*Abl*$^{flox/flox}$ *LysM-Cre*$^{+}$ mice are either on a pure C57BL/6
451 background (SYK)(*17*) or have been backcrossed to C57BL/6 mice at least 5 times
452 (Abl/Arg) (*15*), (*16*). All the experiments involving knockout mice were conducted
453 with WT littermates to ensure control for their genetic background. The Institutional
454 Animal Care and Use Committee at University of Texas Southwestern Medical
455 Center provided approval for all experimental protocols.

456

457 **Mammalian cell culture.** RAW 264.7 cells (ATCC, Manassas, VA) were cultured in
458 Dulbecco's modified Eagle's medium (DMEM) plus 10% endotoxin-free, heat-
459 inactivated, fetal bovine serum (FBS) (GeminiBio, Sacramento, CA) and 1%
460 penicillin–streptomycin as described previously (*15*). For experiments with BMDM,
461 cells were obtained from the humeri, tibias, and femurs of wild type (*WT),* *Syk*$^{flox/flox}$
462 *Cre*$^{+}$, or *Arg*$^{-/-}$*Abl*$^{flox/flox}$ *LysM-Cre*$^{+}$ mice. They were differentiated to *WT, SYK*$^{-/-}$, and
463 *Arg*$^{-/-}$*Abl*$^{-/-}$ BMDM by culturing them in DMEM, 10% FBS, and 20% L929 cell
464 supernatant over 7 days. Differentiation to Mϕ was confirmed (*16*) and samples were
465 screened for *Mycoplasma* contamination (*52*).

466

467 **Parasite culture.** *Leishmania amazonensis* promastigotes (strain
468 IFLA/BR/67/PH8, provided by Norma W. Andrews, University of Maryland,
469 College Park, MD) were maintained at 26°C in Schneider's Drosophila medium
470 (Sigma, S9895, St. Louis, MO) plus 15% FBS and 1% penicillin–streptomycin

471 (*15, 16*). *L. amazonensis* amastigotes were grown axenically at 32°C in
472 Schneider's Drosophila medium at pH 5.5, plus 20% FBS, 1% penicillin–
473 streptomycin, 0.1% hemin (25 mg/mL in 50% triethanolamine), 10 mM adenine, 5
474 mM L-glutamine, 0.25% glucose, 0.5% trypticase, and 40 mM sodium succinate
475 (all from Sigma) (*15, 16*). For uptake (internalization of amastigotes and
476 promastigotes) assays, promastigotes were incubated for 7 days to maximize
477 infective metacyclics (i.e., those isolated through a step Percoll gradient; Sigma).
478 Amastigotes were grown axenically for 5-7 days (*16*). To assess for amastigote
479 growth and replication defects during incubation in MEK/ERK activators or
480 inhibitors, medium containing 10 μM trametinib (Selleck Chemicals, Houston,
481 TX), PMA (Selleck Chemicals), or 0.1% Dimethyl sulfoxide (DMSO, Sigma) was
482 used. To ensure infectivity, parasites were periodically passed in C57/BL6 mice
483 prior to isolation of amastigotes from footpad lesions. A transgenic mNeonGreen
484 expressing line of *L. amazonensis* parasites (*L. amazonensis*-mNeon),
485 containing a marker for hygromycin resistance, was generated (*17*). *L.*
486 *amazonensis*-mNeon promastigotes and amastigotes were maintained as above,
487 but the media was supplemented with 100 μg/mL hygromycin (Sigma). *L.*
488 *amazonensis* virulence was maintained by passage in C57BL/6 mice (*16*). *L.*
489 *amazonensis*-mNeonGreen parasites were detected with an excitation
490 wavelength of 490–494 nm and emission of LP 515 nm.
491
492 **Leishmania uptake assays.** Experiments were adapted and modified as described
493 previously (*15, 16*). BMDMs (*WT, Syk*$^{flox/flox}$ *Cre*$^{+}$, *Arg*$^{-/-}$*Abl*$^{flox/flox}$ *LysM-Cre*$^{+}$) or RAW

494 264.7 cells were plated and treated with inhibitors (imatinib [Arg/Abl inhibitor],
495 PD0325901 [MEK1/2 inhibitor], SCH772984 [ERK1/2 inhibitor], trametinib [MEK1/2
496 inhibitor]) (Selleck Chemicals, Houston, TX), PMA [ERK1/2 activator] or DMSO,
497 where appropriate. Metacyclic promastigotes were incubated in fresh mouse serum
498 for C3bi opsonization, and amastigotes were coated with anti-P8-proteoglycolipid
499 complex (monoclonal antibody IgG1) (*53*). Next, samples with RAW 264.7 cells or
500 BMDMs were incubated with C3bi-opsonized promastigotes at 10 parasites to 1 Mϕ
501 or with IgG-opsonized amastigotes at 10 parasites to 1 Mϕ for 2 h, unless otherwise
502 indicated, and fixed with 3% formaldehyde for 20 minutes. Mouse anti-gp46 antibody
503 was allowed to bind to external promastigotes, whereas mouse anti-P8 antibody was
504 incubated with external amastigotes, as described previously (*15, 16*). Samples
505 were then incubated with Alexa-Fluor-568-conjugated donkey anti-mouse-IgG
506 secondary antibody. All antibodies are listed in **Supplemental Table 3**. This three-
507 color immunofluorescence assay (*54*) allowed distinguishing of internal (green) and
508 external *L. amazonensis* promastigotes or amastigotes (green + red).
509
510 For quantification, samples were imaged with a BioTek Cytation 5 (Agilent, Santa
511 Clara, CA) confocal imaging reader using a 40x objective lens with automated
512 analysis performed (*15*). At least 16 randomly selected fields were automatically
513 visualized per well with each field assessing the number of Mϕ and amastigotes or
514 promastigotes (internalized versus external). The absolute phagocytic index (the
515 number of internalized amastigotes or promastigotes per 100 Mϕ) and normalized
516 adhesion index (the total number of amastigotes or promastigotes per 100 Mϕ) was

517 calculated for each condition. The absolute phagocytic index for DMSO-treated
518 conditions (control) was taken as the maximum value (100%) for each experiment,
519 and phagocytic index for imatinib, SCH772984, trametinib, or PMA-treated samples
520 was determined and normalized relative to that of the control. Means ± SD were
521 calculated. Each experiment was performed with at least 3 biological repeats and
522 contained 3 technical replicates. A one-sample Student's *t*-test or two-way ANOVA
523 was used to determine statistical significance, where appropriate. The representative
524 images shown were visualized using a Biotek Cytation 5 imaging multimode reader.
525 Parasites in representative images were selected from files and linearly processed in
526 Adobe Photoshop CS6 (version 13.0.6).
527
528 **Phagocytosis of beads.** Experiments were adapted and modified as described
529 previously (*15, 16*). RAW 264.7 cells were plated at 70% confluence and incubated
530 overnight in serum-free medium. Except where indicated, samples were pre-
531 incubated in medium containing 3.3 μM imatinib, 1 μM SCH772984, 1 μM trametinib,
532 250 nM PMA or 0.1% DMSO for 1-2 hours. Next, latex yellow–green 2 μm beads
533 (Sigma) were coated with human IgM (Sigma, Cat. #: I-8260) and incubated in rabbit
534 anti-IgM (Sigma, Cat. #: 270A) for IgG opsonization (confirmed as described
535 previously (*16*)). Mϕ were incubated with 10–15 beads/ Mϕ for 2 hours, unless
536 otherwise stated, at 37°C. They were fixed with 3% formaldehyde for 20 minutes,
537 blocked using 2% BSA in PBS (no permeabilization), and then incubated with rabbit
538 anti-human IgM and Hoechst 33258 dye (Sigma) to visualize nuclei. Next, samples
539 were incubated with an Alexa-Fluor-568-conjugated goat anti-rabbit-IgG secondary

540 antibody (Invitrogen, Cat.#: A11034). All antibodies are listed in **Supplemental**
541 **Table 3**. This multi-color immunofluorescence assay (*54*) allowed distinguishing of
542 internalized (green) and external beads (green + red). Quantification was done as
543 above with BioTek Cytation 5 confocal imaging reader using a 40x objective lens
544 with automated analysis performed by the Cytation 5.
545
546 **Western Blot**. To analyze protein/phosphoprotein expression, western blotting was
547 performed. Briefly, RAW264.7 cells or BMDMs from *WT, Syk*$^{flox/flox}$ *Cre*$^{+}$, or
548 *Arg*$^{-/-}$*Abl*$^{flox/flox}$ *LysM-Cre*$^{+}$ mice were incubated overnight in serum-free media (RAW
549 264.7 cells) or L929-free media (BMDM). Experiments were performed at ~70%
550 confluence. Where appropriate, Mϕ were pre-incubated in imatinib, entospletinib,
551 PD0325901, selumetinib, SCH772984, trametinib, PMA or DMSO. IgG-opsonized
552 amastigotes or IgG-opsonized beads were added to adherent starved Mϕ for 30
553 minutes, unless otherwise indicated (*53*), and cells lysed with RIPA extraction buffer
554 and halt protease and phosphatase inhibitor (Thermo Scientific, Cat. #: 78440,
555 Richardson, TX). Protein purity and concentration were addressed using Coomassie
556 Blue staining and BCA assay, respectively, following the manufacturers' protocols.
557 Total proteins were resolved by polyacrylamide gel electrophoresis (12% gels) and
558 transferred to PVDF membranes (BioRad). The membranes were blocked in 5%
559 non-fat dry milk in Tris-buffered saline (TBS) (20 mM Tris at pH 7.6, 150 mM NaCl).
560 The membrane was incubated overnight at 4˚C with the primary antibody in 5% BSA
561 and TBS-T. Next, horseradish peroxidase (HRP)-conjugated anti-mouse secondary
562 antibody (#7076, Cell Signaling Technology) was added at 1:5000 in 5% non-fat dry

563 milk in TBS-T for 1 h. All antibodies are provided in **Supplemental Table 3**.
564 Membranes were incubated in SuperSignal West Pico Chemiluminescent Substrate
565 (Thermo Scientific) for 5 minutes and visualized by using a phosphorimager
566 (ImageQuant LAS 4000, GE Healthcare). For analysis, relative amounts of
567 phosphorylated proteins were compared to total proteins with ImageJ analysis
568 software (https://imagej.nih.gov/ij; membranes were stripped and reprobed). Each
569 experiment had at least 3 biological replicates. Two-way ANOVA was used for
570 statistical tests.
571
572 ***Leishmania* animal model.** For the mouse footpad model of cutaneous
573 leishmaniasis, 10 female C57BL/6 mice per group were infected between 6 and 8
574 weeks of age as previously described (*15, 16*). Briefly, 1×10^6 metacyclic
575 promastigotes were suspended in PBS and injected subcutaneously in the dorsal
576 side of the right hind foot. For the experiments in Fig 6A-C, mice were provided 2
577 mg/kg body weight of trametinib or drug vehicle (4% DMSO and 1% corn oil) by oral
578 gavage daily starting a week before infection and continuing until the mice were
579 euthanized. Two independent experiments were performed. For the experiments in
580 Fig 6D-F, mice were provided 2 mg/kg body weight of trametinib or drug vehicle by
581 oral gavage daily starting 6 weeks after infection and continuing until the mice were
582 euthanized. Lesion growth was documented with calipers every other week by an
583 investigator who was blinded to condition. The ratio of the infected: uninfected foot
584 size was obtained (*55*). ANOVA was used to compare diluent and trametinib-treated
585 mouse groups to swelling at time 0. The number of parasites in lesions was

586 determined by limiting dilution upon termination of the experiment between weeks 14
587 to 16 (*43*).
588
589 Lymph nodes from infected diluent versus trametinib-treated mice were obtained for
590 cytokine and chemokine profiling (*42, 43*). Briefly, lymph node cells were incubated
591 in RPMI 1640 (Invitrogen) plus 10% heat-inactivated FBS, 5×10^{-5} M 2-
592 mercaptoethanol (Sigma), and 1% penicillin-streptomycin. Cells were stimulated with
593 promastigote lysates (equivalent to 1×10^6 or 1×10^5 parasites per sample, as
594 indicated) or concanavalin A (ConA) (5 μg/ml; Sigma). Supernatants were harvested
595 at 72 h and the levels of the cytokines and chemokines IL-4, IL-10, IL-12, IL-13, IL-
596 17, IFN-γ, IL-1β, IL-1α, IP-10, MIP-1α (CCL3), MIP-2 (CXCL2), CXCL9, RANTES
597 (CCL5), and MIP-1β (CCL4) were profiled using the custom multiplex Luminex
598 Platform (R&D Systems, Inc, Minneapolis, MN) through the UT Southwestern
599 Microarray Core as described previously (*56, 57*). Background cytokine levels were
600 calculated using unstimulated supernatants.
601

602 **REFERENCES AND NOTES**:

603 1. S. M. Gossage, M. E. Rogers, P. A. Bates, Two separate growth phases during
604 the development of *Leishmania* in sand flies: implications for understanding the life
605 cycle. *Int J Parasitol* **33**, 1027-1034 (2003).

606 2. W. H. Markle, K. Makhoul, Cutaneous leishmaniasis: recognition and treatment.
607 *Am Fam Physician* **69**, 1455-1460 (2004).

608 3. L. I. McCall, W. W. Zhang, G. Matlashewski, Determinants for the development of
609 visceral leishmaniasis disease. *PLoS Pathog* **9**, e1003053 (2013).

610 4. S. P. Georgiadou, K. P. Makaritsis, G. N. Dalekos, Leishmaniasis revisited: Current
611 aspects on epidemiology, diagnosis and treatment. *J Transl Int Med* **3**, 43-50
612 (2015).

613 5. D. Steverding, The history of leishmaniasis. *Parasit Vectors* **10**, 82 (2017).

614 6. C. Gonzalez, O. Wang, S. E. Strutz, C. Gonzalez-Salazar, V. Sanchez-Cordero,
615 S. Sarkar, Climate change and risk of leishmaniasis in North America: predictions
616 from ecological niche models of vector and reservoir species. *PLoS Negl Trop Dis*
617 **4**, e585 (2010).

618 7. B. E. McIlwee, S. E. Weis, G. A. Hosler, Incidence of endemic human cutaneous
619 leishmaniasis in the United States. *JAMA Dermatol* **154**, 1032-1039 (2018).

620 8. S. L. Croft, S. Sundar, A. H. Fairlamb, Drug resistance in leishmaniasis. *Clin*
621 *Microbiol Rev* **19**, 111-126 (2006).

622 9. E. K. Elmahallawy, A. Agil, Treatment of leishmaniasis: a review and assessment
623 of recent research. *Curr Pharm Des* **21**, 2259-2275 (2015).

624 10. S. Mann, K. Frasca, S. Scherrer, A. F. Henao-Martinez, S. Newman, P. Ramanan,
625 J. A. Suarez, A review of leishmaniasis: current knowledge and future directions.
626 *Curr Trop Med Rep* **8**, 121-132 (2021).
627 11. A. Ponte-Sucre, F. Gamarro, J. C. Dujardin, M. P. Barrett, R. Lopez-Velez, R.
628 Garcia-Hernandez, A. W. Pountain, R. Mwenechanya, B. Papadopoulou, Drug
629 resistance and treatment failure in leishmaniasis: A 21st century challenge. *PLoS*
630 *Negl Trop Dis* **11**, e0006052 (2017).
631 12. E. Handman, D. V. Bullen, Interaction of *Leishmania* with the host macrophage.
632 *Trends Parasitol* **18**, 332-334 (2002).
633 13. J. Alexander, D. G. Russell, The interaction of *Leishmania* species with
634 macrophages. *Adv Parasitol* **31**, 175-254 (1992).
635 14. P. E. Kima, The amastigote forms of *Leishmania* are experts at exploiting host cell
636 processes to establish infection and persist. *Int J Parasitol* **37**, 1087-1096 (2007).
637 15. D. M. Wetzel, E. L. Rhodes, S. Li, D. McMahon-Pratt, A. J. Koleske, The Src
638 kinases Hck, Fgr and Lyn activate Arg to facilitate IgG-mediated phagocytosis and
639 *Leishmania* infection. *J Cell Sci* **129**, 3130-3143 (2016).
640 16. D. M. Wetzel, D. McMahon-Pratt, A. J. Koleske, The Abl and Arg kinases mediate
641 distinct modes of phagocytosis and are required for maximal *Leishmania* infection.
642 *Mol Cell Biol* **32**, 3176-3186 (2012).
643 17. I. Ullah, U. Barrie, R. M. Kernen, E. T. Mamula , A. Datta, L. M. Booshehri, R. E.L.,
644 J. M. Bradford, D. M. Wetzel, The Src and Abl family kinases activate the Spleen
645 Tyrosine Kinase to maximize phagocytosis and *Leishmania* infection. *J Cell Sci.*
646 *BIORXIV/2022/513575*, (2022).

647 18. Z. Yang, D. M. Mosser, X. Zhang, Activation of the MAPK, ERK, following
648 *Leishmania amazonensis* infection of macrophages. *J Immunol* **178**, 1077-1085
649 (2007).
650 19. M. A. Ortiz, T. Mikhailova, X. Li, B. A. Porter, A. Bah, L. Kotula, Src family kinases,
651 adaptor proteins and the actin cytoskeleton in epithelial-to-mesenchymal
652 transition. *Cell Commun Signal* **19**, 67 (2021).
653 20. D. Cortez, G. Reuther, A. M. Pendergast, The Bcr-Abl tyrosine kinase activates
654 mitogenic signaling pathways and stimulates G1-to-S phase transition in
655 hematopoietic cells. *Oncogene* **15**, 2333-2342 (1997).
656 21. A. Jin, T. Kurosu, K. Tsuji, D. Mizuchi, A. Arai, H. Fujita, M. Hattori, N. Minato, O.
657 Miura, BCR/ABL and IL-3 activate Rap1 to stimulate the B-Raf/MEK/Erk and Akt
658 signaling pathways and to regulate proliferation, apoptosis, and adhesion.
659 *Oncogene* **25**, 4332-4340 (2006).
660 22. S. Yang, G. Liu, Targeting the Ras/Raf/MEK/ERK pathway in hepatocellular
661 carcinoma. *Oncol Lett* **13**, 1041-1047 (2017).
662 23. Y. J. Guo, W. W. Pan, S. B. Liu, Z. F. Shen, Y. Xu, L. L. Hu, ERK/MAPK signalling
663 pathway and tumorigenesis. *Exp Ther Med* **19**, 1997-2007 (2020).
664 24. S. T. Eblen, Extracellular-Regulated Kinases: signaling from Ras to ERK
665 substrates to control biological outcomes. *Adv Cancer Res* **138**, 99-142 (2018).
666 25. A. D. Verin, F. Liu, N. Bogatcheva, T. Borbiev, M. B. Hershenson, P. Wang, J. G.
667 Garcia, Role of Ras-dependent ERK activation in phorbol ester-induced
668 endothelial cell barrier dysfunction. *Am J Physiol Lung Cell Mol Physiol* **279**, L360-
669 370 (2000).

670 26. P. A. Martinez, C. A. Petersen, Chronic infection by *Leishmania* amazonensis
671 mediated through MAPK ERK mechanisms. *Immunol Res* **59**, 153-165 (2014).
672 27. M. Shadab, N. Ali, Evasion of Host Defence by *Leishmania donovani*: Subversion
673 of Signaling Pathways. *Mol Biol Int* **2011**, 343961 (2011).
674 28. M. Olivier, D. J. Gregory, G. Forget, Subversion mechanisms by which *Leishmania*
675 parasites can escape the host immune response: a signaling point of view. *Clin*
676 *Microbiol Rev* **18**, 293-305 (2005).
677 29. H. W. Ghalib, J. A. Whittle, M. Kubin, F. A. Hashim, A. M. el-Hassan, K. H.
678 Grabstein, G. Trinchieri, S. G. Reed, IL-12 enhances Th1-type responses in
679 human *Leishmania donovani* infections. *J Immunol* **154**, 4623-4629 (1995).
680 30. S. Bhardwaj, N. Srivastava, R. Sudan, B. Saha, *Leishmania* interferes with host
681 cell signaling to devise a survival strategy. *J Biomed Biotechnol* **2010**, 109189
682 (2010).
683 31. R. M. Mukbel, C. Patten, Jr., K. Gibson, M. Ghosh, C. Petersen, D. E. Jones,
684 Macrophage killing of *Leishmania amazonensis* amastigotes requires both nitric
685 oxide and superoxide. *Am J Trop Med Hyg* **76**, 669-675 (2007).
686 32. T. C. Calegari-Silva, R. M. Pereira, L. D. De-Melo, E. M. Saraiva, D. C. Soares, M.
687 Bellio, U. G. Lopes, NF-kappaB-mediated repression of iNOS expression in
688 *Leishmania amazonensis* macrophage infection. *Immunol Lett* **127**, 19-26 (2009).
689 33. P. M. Boggiatto, P. A. Martinez, A. Pullikuth, D. E. Jones, B. Bellaire, A. Catling,
690 C. Petersen, Targeted extracellular signal-regulated kinase activation mediated by
691 *Leishmania amazonensis* requires MP1 scaffold. *Microbes Infect* **16**, 328-336
692 (2014).

693 34. G. S. Falchook, K. D. Lewis, J. R. Infante, M. S. Gordon, N. J. Vogelzang, D. J.
694 DeMarini, P. Sun, C. Moy, S. A. Szabo, L. T. Roadcap, V. G. Peddareddigari, P.
695 F. Lebowitz, N. T. Le, H. A. Burris, 3rd, W. A. Messersmith, P. J. O'Dwyer, K. B.
696 Kim, K. Flaherty, J. C. Bendell, R. Gonzalez, R. Kurzrock, L. A. Fecher, Activity of
697 the oral MEK inhibitor trametinib in patients with advanced melanoma: a phase 1
698 dose-escalation trial. *Lancet Oncol* **13**, 782-789 (2012).
699 35. Y. Cheng, H. Tian, Current development status of MEK inhibitors. *Molecules* **22**,
700 (2017).
701 36. D. J. Wong, L. Robert, M. S. Atefi, A. Lassen, G. Avarappatt, M. Cerniglia, E.
702 Avramis, J. Tsoi, D. Foulad, T. G. Graeber, B. Comin-Anduix, A. Samatar, R. S.
703 Lo, A. Ribas, Antitumor activity of the ERK inhibitor SCH772984 [corrected] against
704 BRAF mutant, NRAS mutant and wild-type melanoma. *Mol Cancer* **13**, 194 (2014).
705 37. L. Ciuffreda, D. Del Bufalo, M. Desideri, C. Di Sanza, A. Stoppacciaro, M. R.
706 Ricciardi, S. Chiaretti, S. Tavolaro, B. Benassi, A. Bellacosa, R. Foa, A. Tafuri, F.
707 Cognetti, A. Anichini, G. Zupi, M. Milella, Growth-inhibitory and antiangiogenic
708 activity of the MEK inhibitor PD0325901 in malignant melanoma with or without
709 BRAF mutations. *Neoplasia* **11**, 720-731 (2009).
710 38. Y. Sun, W. Z. Liu, T. Liu, X. Feng, N. Yang, H. F. Zhou, Signaling pathway of
711 MAPK/ERK in cell proliferation, differentiation, migration, senescence and
712 apoptosis. *J Recept Signal Transduct Res* **35**, 600-604 (2015).
713 39. M. T. Crowley, P. S. Costello, C. J. Fitzer-Attas, M. Turner, F. Meng, C. Lowell, V.
714 L. Tybulewicz, A. L. DeFranco, A critical role for Syk in signal transduction and

715 phagocytosis mediated by Fcgamma receptors on macrophages. *J Exp Med* **186**,
716 1027-1039 (1997).
717 40. F. Kiefer, J. Brumell, N. Al-Alawi, S. Latour, A. Cheng, A. Veillette, S. Grinstein, T.
718 Pawson, The Syk protein tyrosine kinase is essential for Fcgamma receptor
719 signaling in macrophages and neutrophils. *Mol Cell Biol* **18**, 4209-4220 (1998).
720 41. S. Ramanathan, J. A. Di Paolo, F. Jin, L. Shao, S. Sharma, M. Robeson, B. P.
721 Kearney, Pharmacokinetics, pharmacodynamics, and safety of entospletinib, a
722 novel pSYK inhibitor, following single and multiple oral dosing in healthy
723 volunteers. *Clin Drug Investig* **37**, 195-205 (2017).
724 42. L. Soong, C. A. Henard, P. C. Melby, Immunopathogenesis of non-healing
725 American cutaneous leishmaniasis and progressive visceral leishmaniasis. *Semin*
726 *Immunopathol* **34**, 735-751 (2012).
727 43. L. Soong, C. H. Chang, J. Sun, B. J. Longley, Jr., N. H. Ruddle, R. A. Flavell, D.
728 McMahon-Pratt, Role of CD4+ T cells in pathogenesis associated with *Leishmania*
729 *amazonensis* infection. *J Immunol* **158**, 5374-5383 (1997).
730 44. P. M. Boggiatto, F. Jie, M. Ghosh, K. N. Gibson-Corley, A. E. Ramer-Tait, D. E.
731 Jones, C. A. Petersen, Altered dendritic cell phenotype in response to *Leishmania*
732 *amazonensis* amastigote infection is mediated by MAP kinase, ERK. *Am J Pathol*
733 **174**, 1818-1826 (2009).
734 45. N. Ueno, M. E. Wilson, Receptor-mediated phagocytosis of *Leishmania*:
735 implications for intracellular survival. *Trends Parasitol* **28**, 335-344 (2012).
736 46. K. L. Cheeseman, T. Ueyama, T. M. Michaud, K. Kashiwagi, D. Wang, L. A. Flax,
737 Y. Shirai, D. J. Loegering, N. Saito, M. R. Lennartz, Targeting of protein kinase C-

738 epsilon during Fcgamma receptor-dependent phagocytosis requires the
739 epsilonC1B domain and phospholipase C-gamma1. *Mol Biol Cell* **17**, 799-813
740 (2006).
741 47. E. C. Larsen, T. Ueyama, P. M. Brannock, Y. Shirai, N. Saito, C. Larsson, D.
742 Loegering, P. B. Weber, M. R. Lennartz, A role for PKC-epsilon in Fc gammaR-
743 mediated phagocytosis by RAW 264.7 cells. *J Cell Biol* **159**, 939-944 (2002).
744 48. T. S. Panetti, S. A. Wilcox, C. Horzempa, P. J. McKeown-Longo, Alpha v beta 5
745 integrin receptor-mediated endocytosis of vitronectin is protein kinase C-
746 dependent. *J Biol Chem* **270**, 18593-18597 (1995).
747 49. N. Roy, S. Chakraborty, B. Paul Chowdhury, S. Banerjee, K. Halder, S. Majumder,
748 S. Majumdar, P. C. Sen, Regulation of PKC mediated signaling by calcium during
749 visceral leishmaniasis. *PLoS One* **9**, e110843 (2014).
750 50. A. Zheleznyak, E. J. Brown, Immunoglobulin-mediated phagocytosis by human
751 monocytes requires protein kinase C activation. Evidence for protein kinase C
752 translocation to phagosomes. *J Biol Chem* **267**, 12042-12048 (1992).
753 51. J. S. Arthur, S. C. Ley, Mitogen-activated protein kinases in innate immunity. *Nat*
754 *Rev Immunol* **13**, 679-692 (2013).
755 52. C. C. Uphoff, H. G. Drexler, Eradication of mycoplasma contaminations. *Methods*
756 *Mol Biol* **946**, 15-26 (2013).
757 53. A. A. Pan, D. McMahon-Pratt, Monoclonal antibodies specific for the amastigote
758 stage of Leishmania pifanoi. I. Characterization of antigens associated with stage-
759 and species-specific determinants. *J Immunol* **140**, 2406-2414 (1988).

760 54. D. M. Wetzel, S. Hakansson, K. Hu, D. Roos, L. D. Sibley, Actin filament
761 polymerization regulates gliding motility by apicomplexan parasites. *Mol Biol Cell*
762 **14**, 396-406 (2003).
763 55. J. Champsi, D. McMahon-Pratt, Membrane glycoprotein M-2 protects against
764 *Leishmania amazonensis* infection. *Infect Immun* **56**, 3272-3279 (1988).
765 56. A. Navas, D. A. Vargas, M. Freudzon, D. McMahon-Pratt, N. G. Saravia, M. A.
766 Gomez, Chronicity of dermal leishmaniasis caused by *Leishmania panamensis* is
767 associated with parasite-mediated induction of chemokine gene expression. *Infect*
768 *Immun* **82**, 2872-2880 (2014).
769 57. L. Gonzalez-Fajardo, O. L. Fernandez, D. McMahon-Pratt, N. G. Saravia, Ex vivo
770 host and parasite response to antileishmanial drugs and immunomodulators. *PLoS*
771 *Negl Trop Dis* **9**, e0003820 (2015).
772

773 **ACKNOWLEDGEMENTS:**

774 **General:** We thank Drs. Neal M. Alto, Melanie H. Cobb, James J. Collins,
775 Margaret A. Phillips, and Michael L. Reese (all at UT Southwestern) for helpful
776 discussions and feedback. Francis Khuong and Catherine Trice provided expert
777 technical assistance and helped to edit this manuscript. Members of the UT
778 Southwestern Departments of Pediatrics, Biochemistry, Microbiology, and
779 Pharmacology provided valuable feedback and permitted common equipment
780 use. Dr. Diane McMahon-Pratt (Yale University) generously donated
781 antileishmanial antibodies. Dr. Anthony J. Koleske (Yale University) provided the
782 *Arg*$^{-/-}$*Abl*$^{flox/flox}$ mice. The UT Southwestern Microarray Core assisted with
783 cytokine/chemokine profiling.

784

785 **Funding:** This work was supported by a Children's Clinical Research Advisory
786 Committee (CCRAC) Junior Investigator Award, a CCRAC Early Investigator
787 Award, the National Institutes of Health (K08 AI103036 and R01 AI146349),
788 Welch Foundation Grant I-2048, and the UT Southwestern Department of
789 Pediatrics (to D.M.W.). U.B. was supported by a National Institutes of Health
790 Supplement to Promote Diversity in Health-Related Research (R01 AI146349-
791 S1) and Medical Scientist Training (MD/PhD) Grant NIH T32GM008014. K.F.
792 was supported by a UT Southwestern-Amgen Summer Research Fellowship.

793

794 **Author contributions:** U.B. and D.M.W. designed and performed experiments,
795 analyzed data, and wrote the manuscript. K.F. conducted experiments, assisted

with data analysis, and edited the manuscript. A.D. helped to design and perform experiments and edited the manuscript.

Competing interests: The authors have no competing financial interests.

Data and materials availability: All data are available within the main text of the manuscript or the supplemental materials. Any materials generated for this manuscript are freely available upon request.

805 **List of figures:**

806 **Figure 1.** The MAPK/ERK pathway is required for optimal amastigote uptake.

807 **Figure 2**. MAPK/ERK are activated during *Leishmania* uptake by Mϕ.

808 **Figure 3.** PMA activates ERK1/2 to modulate amastigote uptake.

809 **Figure 4.** SYK and Arg/Abl stimulate ERK1/2 phosphorylation during amastigote
810 uptake.

811 **Figure 5.** ERK 1/2's role in *Leishmania* uptake is greater than for phagocytosis of
812 beads.

813 **Figure 6.** MAPK/ERK permit efficient infection in a mouse model of cutaneous
814 leishmaniasis.

815 **Table 1.** Ongoing trametinib treatment during *L. amazonensis* infection has
816 limited effects on Th1 vs Th2 responses.

817 **Table 2.** Cytokine and chemokine profiles in diluent versus trametinib-treated,
818 *Leishmania*-infected mice.

819

820 **List of supplementary materials:**

821 **Supplemental Figure 1.** MAPK/ERK facilitate *L. amazonensis* uptake.

822 **Supplemental Table 1.** Trametinib initiated during *L. amazonensis* infection has

823 limited effects on Th1 vs Th2 responses.

824 **Supplemental Table 2.** Cytokine and chemokine profiles from *Leishmania*-

825 infected mice treated once lesions are visible.

826 **Supplemental Table 3.** Antibodies.

827 **FIGURES AND LEGENDS:**

828 **Figure 1**

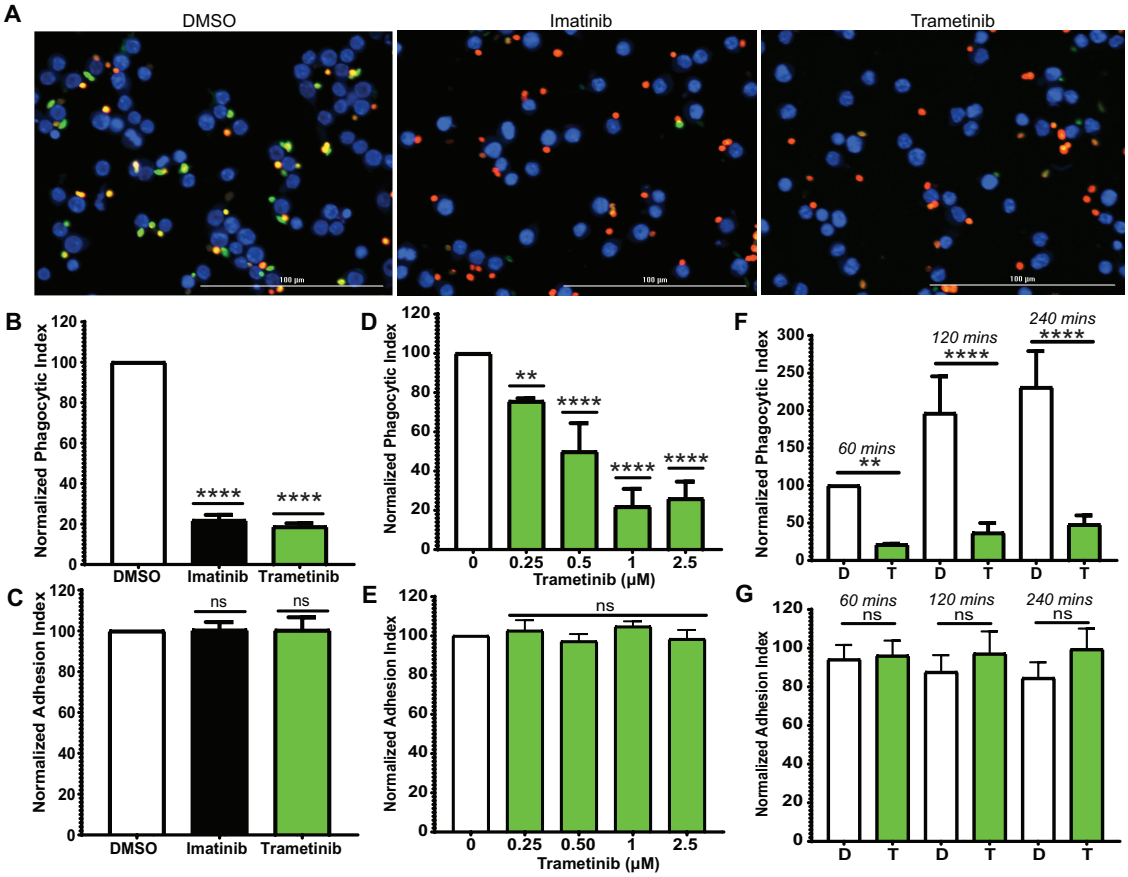

829

830 **Figure 1. The MAPK/ERK pathway is required for optimal amastigote**

831 **uptake. (A)** Trametinib decreases IgG-opsonized amastigote uptake. RAW 264.7

832 cells were treated with 3.3 μM imatinib, 1 μM trametinib or DMSO for 2 h, and 10

833 IgG-opsonized amastigotes were incubated per RAW 264.7 cell for 2 h at 37°C.

834 An immunofluorescence assay distinguished between intracellular (green) and

835 extracellular (red + green) amastigotes. Nuclei are labeled with Hoescht 33342

836 (blue). Scale bar, 100 μm. **(B)** Graph showing the mean phagocytic index (PI) ±

837 standard deviation (SD) for RAW 264.7 cells normalized to DMSO for each

838 experiment (100%), quantified from n = 6 biological experiments. Comparisons

839 between imatinib and trametinib by ANOVA were nonsignificant. **(C)** Imatinib and
840 trametinib do not affect the total (external + internal) number of amastigotes per
841 100 RAW cells (termed an adhesion index). Shown are percentages of total
842 amastigotes per 100 imatinib-treated and trametinib-treated RAW 264.7 cells
843 relative to DMSO-treated cells for the experiment shown in B. **(D)** Titration of
844 trametinib demonstrates that the reduction of amastigote internalization is
845 maximal at ~100x the purified MEK1/2 IC_{50}. RAW 264.7 cells were treated with
846 increasing doses of trametinib (0.25, 0.5, 1, or 2.5 μM) or DMSO. Bar graph
847 shows the mean PI ± SD for trametinib-treated samples relative to DMSO-treated
848 samples for each experiment (100%) for 4 biological experiments. **(E)** The
849 adhesion index for amastigotes from experiment in D is not affected by
850 increasing doses of trametinib. Experiment performed as in C. **(F)** The relative
851 decrease in PI for trametinib-treated samples persists even after prolonged
852 incubation. RAW 264.7 cells were treated with DMSO (D) or 1 μM trametinib (T)
853 prior to addition of IgG-opsonized amastigotes for 1 h, 2 h, or 4 h, as indicated.
854 Shown is the mean PI ± SD for each time point for the trametinib-treated
855 condition, relative to the DMSO-treated condition, calculated from 4 biological
856 experiments. **(G)** Treating samples with trametinib for prolonged periods does not
857 affect the adhesion index for amastigotes. Shown are the total number of
858 amastigotes (internal + external) per 100 RAW 264.7 cells for the experiments
859 performed in F. For all experiments, ** $P < 0.01$, **** $P < 0.0001$, ns =
860 nonsignificant compared to the relevant DMSO-treated category by ANOVA.
861

862 **Figure 2**

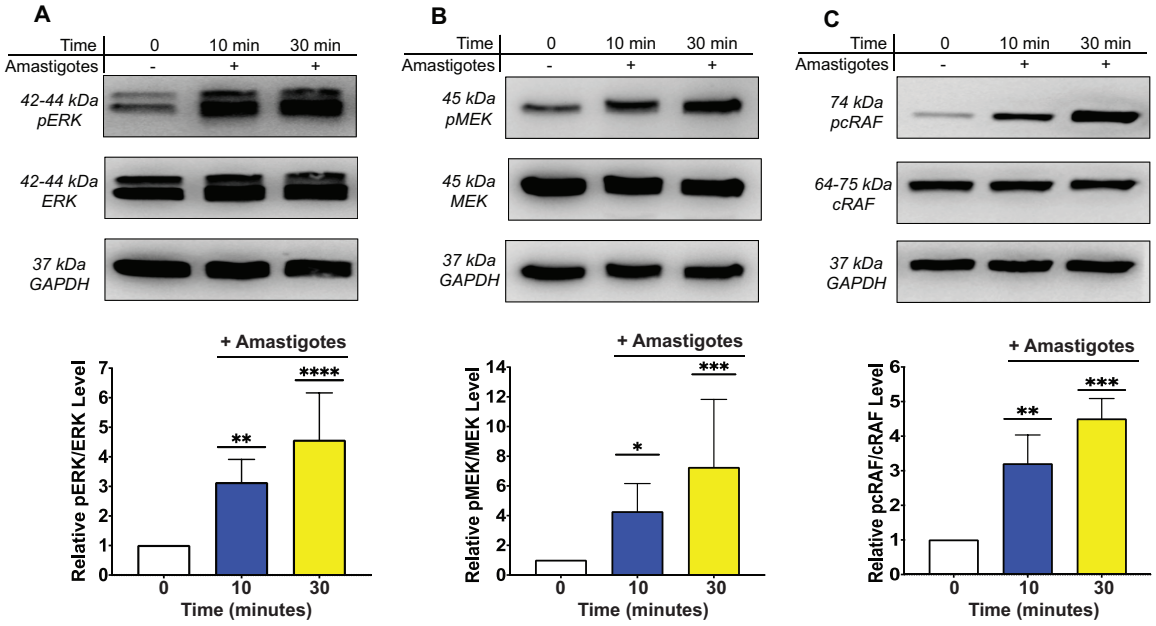

863

864 **Figure 2**. **MAPK/ERK are activated during *Leishmania* uptake by Mϕ.**

865 Amastigotes were added to ≥ 70% confluent RAW 264.7 cells. Equal amounts of

866 protein from whole lysates were employed for each category. **Top:**

867 Representative blots displaying relative activation of MAPK/ERK. Phosphorylated

868 **(A)** ERK1/2, **(B)** MEK1/2, **(C)** cRaf (Raf-1) and the corresponding total proteins

869 were detected by Western Blot. An unrelated protein, GAPDH, is shown as an

870 additional loading control. **Bottom:** Quantification of phosphorylated MAPK/ERK

871 levels. Graphs shown in **(A)** for ERK1/2, **(B)** for MEK1/2, and **(C)** for cRaf

872 represent mean ± SD of relative phosphorylated kinase levels, normalized to total

873 kinase levels, for at least 3 biological replicates per condition. * $P < 0.05$, ** $P <$

874 0.01, *** $P < 0.001$, **** $P < 0.0001$ by ANOVA compared to the 0 m time point

875 for each set of kinases.

876

877 **Figure 3**

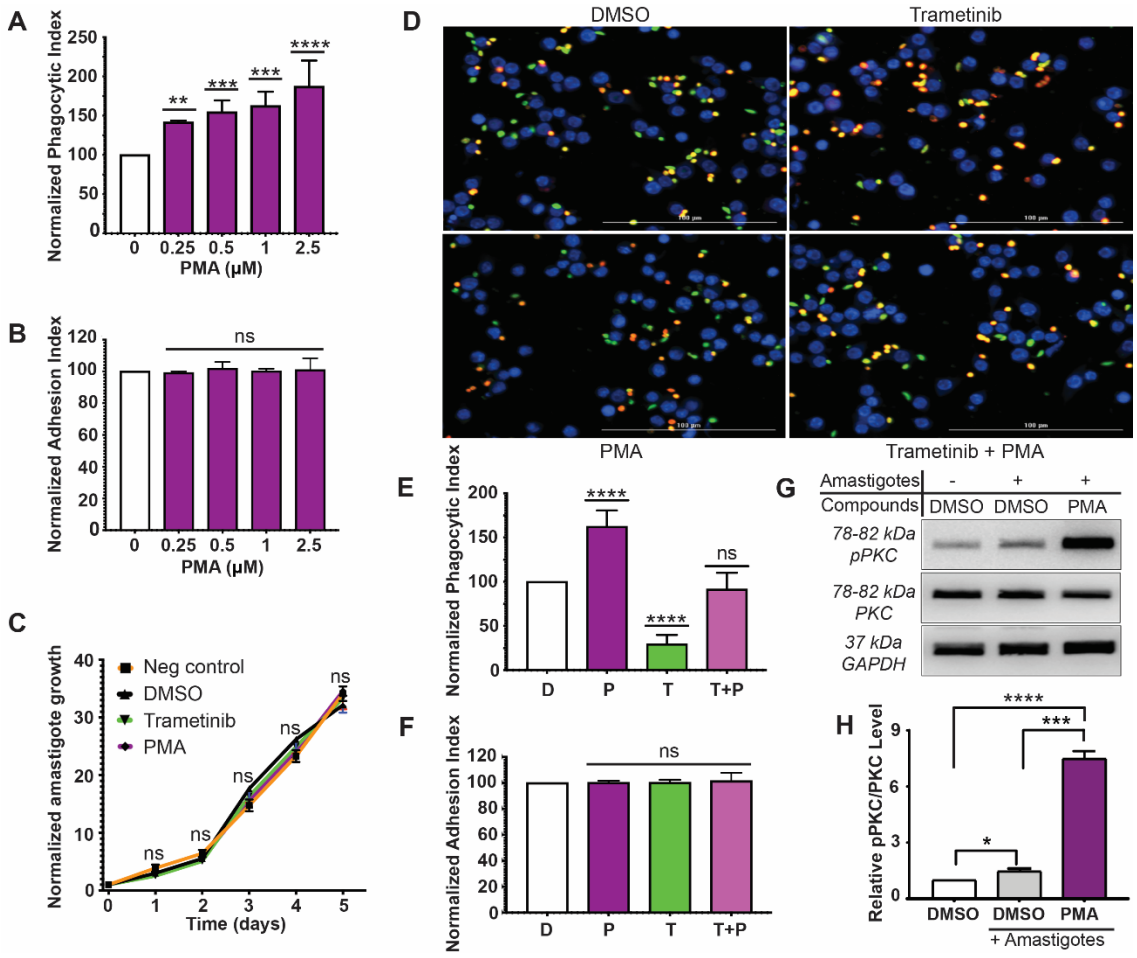

878

879 **Figure 3. PMA activates ERK1/2 to modulate amastigote uptake**. **(A)** PMA
880 increases IgG-opsonized amastigote uptake. BMDM were treated with DMSO or
881 increasing doses of PMA (0.25, 0.5, 1, 2.5 μM) prior to incubation with IgG-
882 opsonized amastigotes for the times indicated. n = 4 experiments. ** $P < 0.01$, ***
883 $P < 0.001$, **** $P < 0.0001$ compared to DMSO category by ANOVA. **(B)** PMA
884 does not affect the adhesion index for amastigotes. ns, not significant by
885 ANOVA. **(C)** Trametinib and PMA are not toxic to amastigotes. Shown is one
886 representative experiment of five experiments with two technical repeats
887 following the number of amastigotes growing in DMSO-treated, PMA-treated, or

888 trametinib-treated media over 5 days relative to on day 0. ns, $P > 0.05$ compared
889 to DMSO category by ANOVA. **(D)** Representative image demonstrating that
890 PMA rescues trametinib inhibition of *Leishmania* amastigote uptake. BMDM were
891 treated with DMSO, 1 μM PMA, 1 μM trametinib or a combination of 1 μM
892 trametinib and 1 μM PMA prior to incubation with IgG-opsonized amastigotes for
893 2 hours. **(E)** Mean PI ± SD for BMDM treated with trametinib/PMA relative to
894 DMSO-treated samples for each experiment (100%), obtained from 3 biological
895 experiments. **** $P < 0.0001$, ns = nonsignificant by ANOVA compared to
896 DMSO-treated sample. **(F)** Trametinib/PMA does not affect amastigote adhesion
897 for the experiment shown in E. **(G, H)** PKC is only slightly activated during
898 amastigote uptake. PMA serves as a positive control. Amastigotes were added to
899 monolayers of RAW 264.7 cells and processed as above. Shown are **(G)**
900 representative blots demonstrating and **(H)** bar graphs quantifying relative
901 activation of pPKC/PKC. * $P < 0.05$, *** $P < 0.001$, **** $P < 0.0001$ compared with
902 samples indicated by brackets (ANOVA). n = 3 experiments.
903

904 **Figure 4**

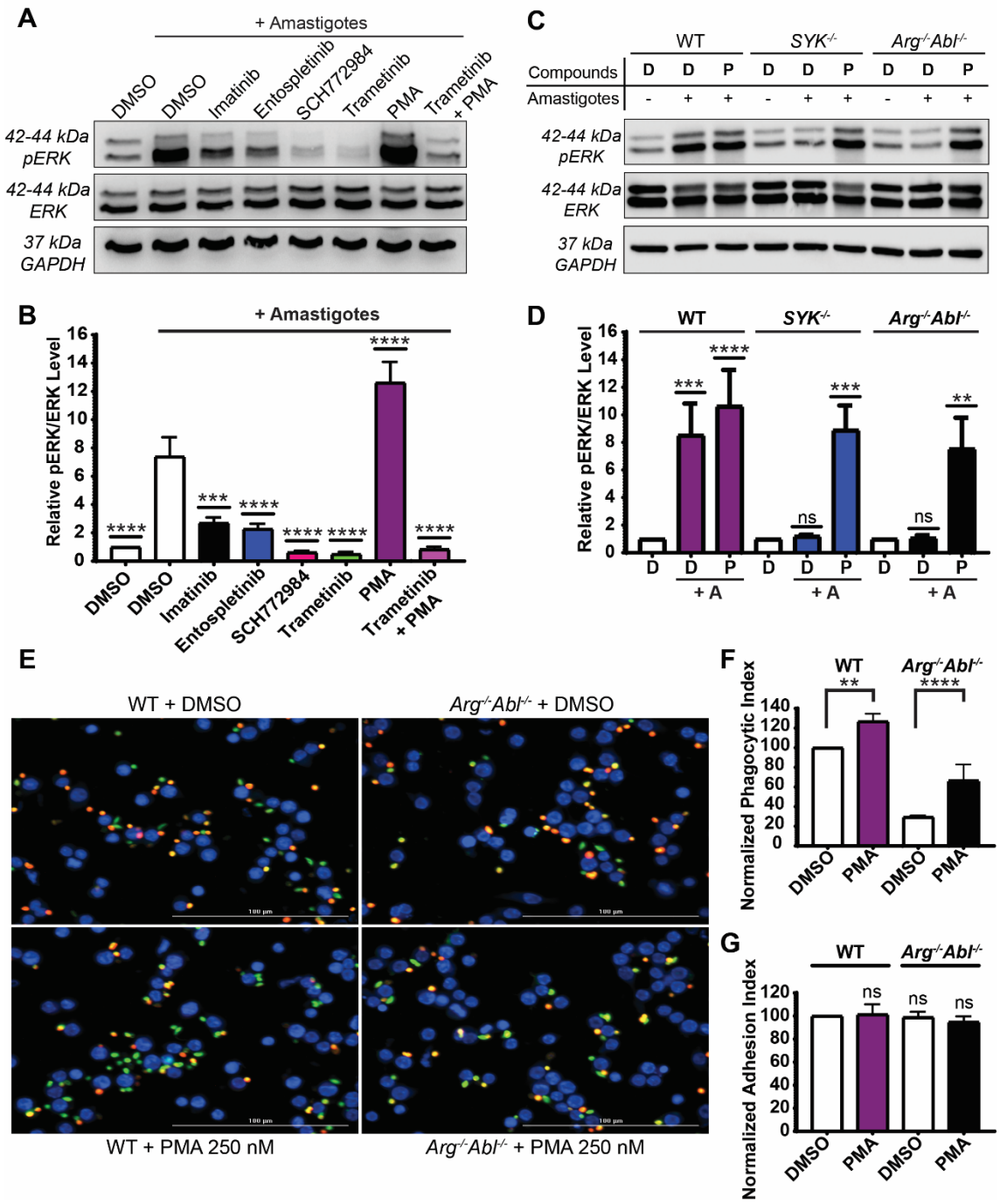

905

906 **Figure 4. SYK and Arg/Abl stimulate ERK1/2 phosphorylation during**

907 **amastigote uptake. (A)** Phosphorylation of ERK1/2 in RAW 264.7 cells is

908 induced upon amastigote uptake and is decreased by imatinib (Arg/Abl inhibitor),

909 entospletinib (SYK inhibitor), SCH772984 (ERK1/2 inhibitor), and trametinib
910 (MEK1/2 inhibitor). PMA serves as a positive control for pERK stimulation. RAW
911 264.7 cells were allowed to adhere to plates, and then treated with compounds or
912 DMSO prior to IgG-opsonized amastigote addition, lysis, and immunoblotting.
913 Representative immunoblots of pERK1/2 (top) and total ERK1/2 (bottom) [with
914 (+) or without (–) amastigotes] are shown. **(B)** Relative pERK levels, normalized
915 to ERK1/2 levels, among categories shown in A. Levels of pERK are normalized
916 to amastigote-exposed DMSO-treated RAW 264.7 cells (100%). 5 biological
917 replicates are quantified. *** $P < 0.001$, **** $P < 0.0001$ compared with
918 amastigote-stimulated, DMSO-treated RAW 264.7 cells (ANOVA). **(C)**
919 Phosphorylation of ERK1/2 induced upon FcγR engagement is decreased
920 in *SYK*$^{-/-}$ and *Arg*$^{-/-}$*Abl*$^{-/-}$ BMDM compared to WT BMDM. Shown is a
921 representative immunoblot of pERK1/2 (top) and total ERK1/2 (bottom) in WT,
922 *SYK*$^{-/-}$ and *Arg*$^{-/-}$*Abl*$^{-/-}$ BMDM treated with DMSO (D) or PMA (P), ± incubation
923 with amastigotes. **(D)** Graph showing relative levels of pERK1/2, normalized to
924 ERK1/2 levels, among WT, *SYK*$^{-/-}$, and *Arg*$^{-/-}$*Abl*$^{-/-}$ BMDM treated with DMSO
925 (D) or PMA (P), ± amastigotes (A). ** $P < 0.01$, *** $P < 0.001$, **** $P < 0.0001$, ns:
926 not significant by ANOVA (n = 6 experiments), compared to DMSO + amastigote
927 category for each condition. **(E-G)** Primary cells lacking Arg and Abl exhibit
928 decreases in amastigote uptake, but PMA can partially rescue this amastigote
929 internalization defect. **(E)** Representative image performed as in Fig 1. **(F)** Mean
930 phagocytic index ± SD for PMA-treated and/or *Arg*$^{-/-}$ *Abl*$^{-/-}$ BMDM relative to WT
931 DMSO-treated BMDM. **(G)** DMSO and PMA do not affect the adhesion indexes

932 for the experiments shown in F. n for F-G = 3 experiments. ** $P < 0.01$; *** $P <$

933 0.001; **** $P < 0.0001$; ns, not significant compared with DMSO-treated WT

934 BMDM (ANOVA).

935

936 **Figure 5**

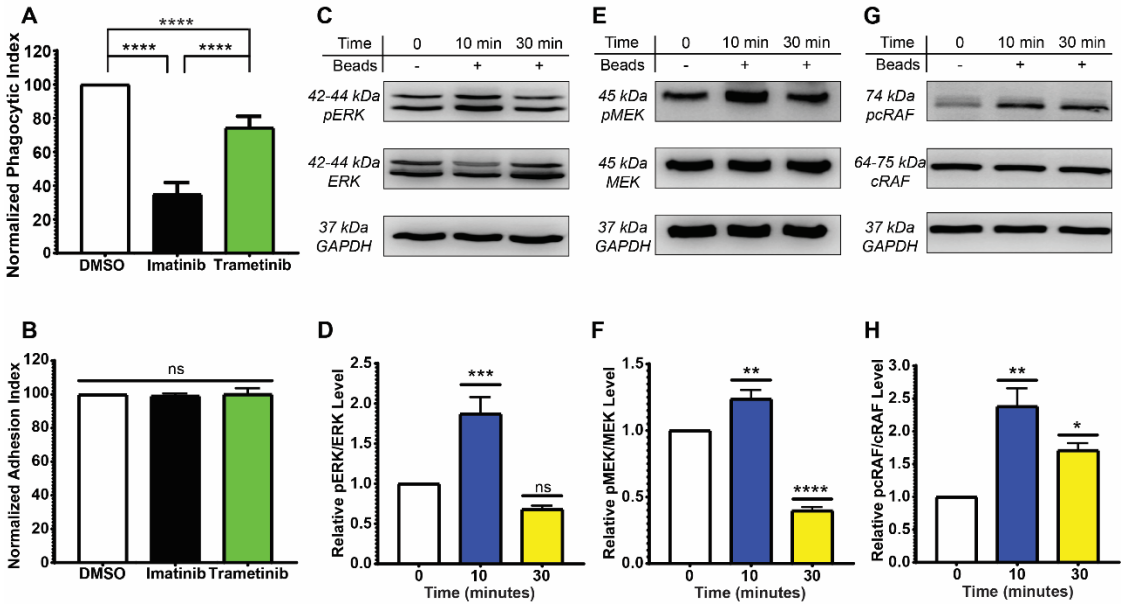

937

938 **Figure 5. ERK 1/2's role in *Leishmania* uptake is greater than for**

939 **phagocytosis of beads**. **(A)** Trametinib mildly decreases bead internalization.

940 RAW 264.7 cells were treated with 3.3 μM imatinib, 1 μM trametinib or DMSO for

941 2 hr. prior to addition of 10 IgG-opsonized beads per RAW 264.7 cell for 2 h at

942 37°C. Treating RAW 264.7 cells with trametinib decreases uptake of IgG-

943 opsonized beads to a lesser degree than imatinib. Graph shows the mean PI ±

944 SD for each category, normalized to DMSO (100%). **** $P < 0.0001$, ns: not

945 significant compared to indicated categories by ANOVA (n = 6 biological

946 experiments). **(B)** Imatinib and trametinib does not affect the adhesion index for

947 beads in the experiments shown in A. **(C-H)** IgG-coated beads activate the

948 MAPK/ERK pathway, but phosphorylation is not sustained. Beads were added to

949 > 70% confluent RAW 264.7 cells and experiments were processed as in Fig 2.

950 Top: Phosphorylated forms of **(C)** ERK, **(E)** MEK1/2, **(G)** cRaf and the

951 corresponding total kinase were detected by Western blotting. Bottom: Relative
952 activation was quantified for **(D)** ERK, **(F)** MEK1/2, and **(H)** cRaf, using the
953 methods described in Fig 2. * $P < 0.05$, ** $P < 0.01$, *** $P < 0.001$, **** $P < 0.0001$
954 and ns: not significant compared to 0 m timepoint by ANOVA ($n \geq 3$
955 experiments).
956

957 **Figure 6**

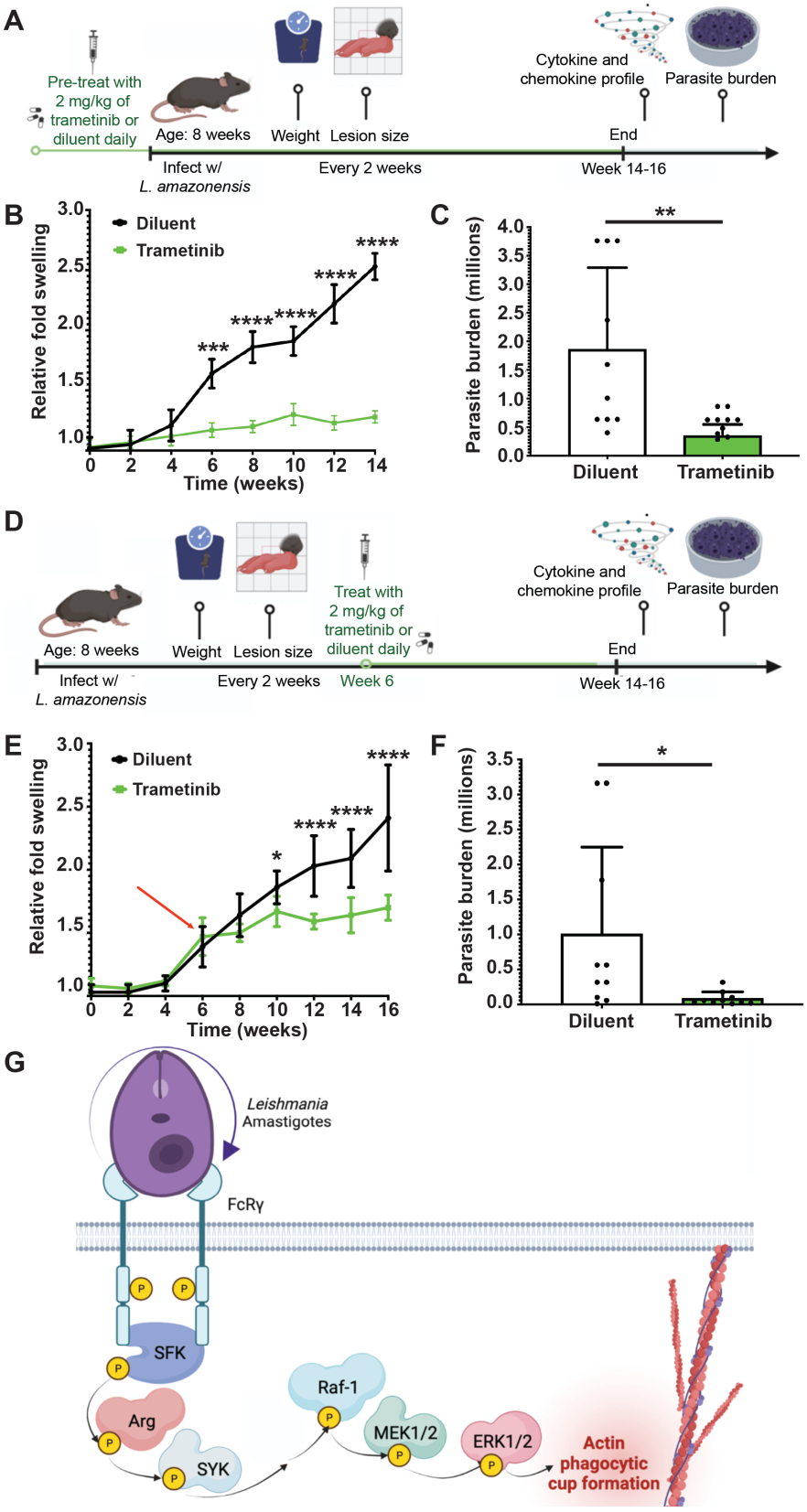

958

959 **Figure 6. MAPK/ERK permit efficient infection in a mouse model of**
960 **cutaneous leishmaniasis. (A)** Mouse footpad model for cutaneous
961 leishmaniasis. C57BL/6 mice diluent and trametinib-treated groups were injected
962 with promastigotes in the hind footpad. Mice were given 2 mg/kg body weight of
963 trametinib or an equal volume of diluent by oral gavage daily, starting 7 days
964 before infection and continuing until the mice were euthanized. Two experiments
965 were performed. Shown in the following panels is one representative experiment
966 containing 10 female mice per group. **(B)** Trametinib given prior to infection
967 reduces lesion size in mice. Depth of foot swelling was monitored with calipers by
968 a blinded investigator. Results represent the mean ± SD foot size increase over
969 the uninfected foot (normalized to 1). The control (diluent) and drug-treated
970 groups were compared to swelling at time 0 by ANOVA; * $P < 0.05$, **** $P <$
971 0.0001, ns, not significant. **(C)** Trametinib given prior to infection significantly
972 reduces parasite burden. Parasite burdens in infected footpads were determined
973 by limiting dilution as described in *Materials and Methods*. Plotted is the mean
974 number of parasites (*i.e*, parasite burden) in millions at the end of the experiment
975 shown in B ± SD. In this example, there were 1.41×10^6 parasites in the control
976 mice versus 2.03×10^5 parasites in the trametinib-treated mice. *$P < 0.05$ (two-
977 tailed *t*-test). **(D)** C57BL/6 mice diluent and trametinib-treated groups were
978 injected with *L. amazonensis* promastigotes as above. Starting 6 weeks after
979 inoculation (arrow), mice were given 2 mg/kg body weight of trametinib or vehicle
980 by oral gavage daily and continuing until the experiment was terminated. **(E)**
981 Trametinib given once lesions have begun reduces lesion size in trametinib-

982 treated mice compared to diluent-treated mice. Arrow shows start time of drug
983 treatment. Shown is one representative experiment containing 10 female mice
984 per group. Statistics calculated as in B. **(F)** Lesions in mice treated with
985 trametinib 6 weeks after infection contain fewer *Leishmania* parasites than
986 control mice. Plotted is the mean ± SD lesion parasite burden in millions at the
987 end of the experiment shown in E; in this example, there were 1.01 x 10^6
988 parasites in the control mice versus 8.29 x 10^4 parasites in the trametinib-treated
989 mice (>10-fold reduction). *P <0.05 (two-tailed t-test). (**G**) MAPK/ERK signal
990 transduction in Mϕ facilitates *Leishmania* uptake and pathogenesis. Upon FcγR
991 ligation by amastigotes, SFK, Arg, and SYK are activated and relay signals to the
992 MAPK/ERK pathway, which leads to phagocytic cup formation and allows the
993 internalization of *Leishmania*. Diagrams created with Biorender.
994

995 **Table 1**

Experiment	Ratio	DMSO - High	Trametinib - High	DMSO - Low	Trametinib - Low
Trametinib prior to infection	**IFN Gamma/IL-4**	1.86	1.35	1.75	1.05
	IFN Gamma/IL-13	0.78	0.11	0.75	0.09
	IFN Gamma/IL-4+ IL-10+ IL-13	0.55	0.10	0.52	0.08

996

997 **Table 1. Ongoing trametinib treatment during *L. amazonensis* infection has**
998 **limited effects on Th1 vs Th2 responses.** Effects of trametinib during *L.*
999 *amazonensis* infection on cytokine secretion. Shown are profiles of draining
1000 lymph nodes isolated from diluent versus trametinib-treated mice treated prior to
1001 inoculation as described in methods. Ratios of IFNγ: IL-4, IFNγ: IL-13, and IFNγ:
1002 IL-4+10+13 were calculated from the data shown in Table 2. Trametinib may
1003 skew towards a Th2 response, which should not promote lesion healing.

1004

1005 **Table 2**

Experiment	Cytokine	Treatment	Cytokine secretion (pg) after					
			Con A stimulation		High stimulation		Low treatment	
			AVG	STD	AVG	STD	AVG	STD
Trametinib prior to infection	**IFN Gamma (38)**	DMSO	6.70	6.83	6.06	5.82	5.83	5.16
		Trametinib	0.48	0.64	0.73	1.05	0.58	0.75
		p-value	**0.01**		**0.01**		**0.005**	
	IL-1 BETA (19)	DMSO	0.88	0.51	0.97	0.48	0.73	0.46
		Trametinib	0.45	0.12	0.42	0.11	0.39	0.09
		p-value	**0.02**		**0.002**		**0.03**	
	IL-12/IL23p40 (64)	DMSO	5.56	2.97	5.24	2.49	6.04	3.06
		Trametinib	3.28	1.18	3.39	0.79	3.53	1.31
		p-value	**0.04**		**0.04**		**0.03**	
	IL-13 (35)	DMSO	5.08	3.04	7.72	2.47	7.78	3.07
		Trametinib	7.01	2.27	6.83	1.10	6.57	1.15
		p-value	NS		NS		NS	
	IL-17A (52)	DMSO	0.48	0.24	0.65	0.14	0.53	0.27
		Trametinib	0.59	0.09	0.74	0.25	0.53	0.25
		p-value	NS		NS		NS	
	IL-4 (26)	DMSO	2.36	1.26	3.26	1.89	3.32	2.57
		Trametinib	0.49	0.64	0.54	0.68	0.55	0.70
		p-value	**0.0006**		**0.0004**		**0.004**	

	TNF ALPHA (45)	DMSO	2.98	1.6	2.68	2.10	2.45	1.22
		Trametinib	2.85	2.30	2.23	0.96	1.75	1.45
		p-value	NS		NS		NS	
	IL-10 (13)	DMSO	.008	.007	.02	.009	.009	.01
		Trametinib	8.94	8.78	8.36	10.44	5.16	1.06
		p-value	**0.005**		**0.02**		**0.0001**	
	MCP-1 (51)	DMSO	25.56	14.87	25.07	12.31	27.90	10.54
		Trametinib	7.23	6.43	7.23	5.87	7.23	6.56
		p-value	**0.002**		**0.0006**		**0.0001**	
	MIP-1 ALPHA (47)	DMSO	4.69	3.95	3.93	2.77	4.62	2.96
		Trametinib	1.36	0.41	1.44	0.86	1.44	0.88
		p-value	**0.02**		**0.01**		**0.004**	

Table 2. Cytokine and chemokine profiles in diluent versus trametinib-treated, *Leishmania*-infected mice. Shown are profiles of draining lymph nodes isolated from DMSO versus trametinib mice treated prior to infection as described in methods. Post 14-16 weeks, mice were sacrificed and multiplex chemokine ELISAs were performed on harvested lymph node supernatants. *P* values were determined by two-tailed t-tests and are listed if $P < 0.1$. Bold: $P \leq 0.05$.